Pharm Res (2012) 29:1404–1418
DOI 10.1007/s11095-011-0628-x

RESEARCH PAPER

Inorganic-Organic Magnetic Nanocomposites for use in Preventive Medicine: A Rapid and Reliable Elimination System for Cesium

Yoshihisa Namiki • Tamami Namiki • Yukiko Ishii • Shigeo Koido • Yuki Nagase • Akihito Tsubota • Norio Tada • Yoshitaka Kitamoto

Received: 14 July 2011 / Accepted: 16 November 2011 / Published online: 7 December 2011

ABSTRACT

Purpose To investigate the potential use of Prussian blue-coated magnetic nanoparticles, termed "Prussian blueberry", to bring about the magnetic elimination of cesium.

Methods Prussian blueberry were prepared by a layer-by-layer assembly method. The morphology, structure and physical properties of the Prussian blueberry were investigated as was their ability to magnetically eliminate cesium.

Results We confirmed that Prussian blueberry were composed of a magnetite nanoparticle-core and a Prussian blue-shell. Under a magnetic field, Prussian blueberry (5 mg) reduced the cesium concentration of seawater (3 ml) from 150 ppm to about 50 ppm; but regular Prussian blue could not magnetically eliminate cesium. Moreover, Prussian blueberry removed a similar proportion of cesium from a larger volume of seawater, and from fetal bovine serum and cow's milk.

Conclusions Under a magnetic field, Prussian blueberry was able to rapidly eliminate cesium from seawater and from biological matrices such as serum and milk.

Y. Namiki (✉) • Y. Ishii • Y. Nagase • A. Tsubota • N. Tada
Institute of Clinical Medicine and Research
The Jikei University School of Medicine
Kashiwa, Japan
e-mail: cancer_gene_therapy@ybb.ne.jp

T. Namiki
Department of Radiology
The Jikei University School of Medicine
Kashiwa, Japan

S. Koido
Division of Gastroenterology and Hepatology
The Jikei University School of Medicine
Kashiwa, Japan

Y. Kitamoto
Department of Innovative and Engineered Materials
Interdisciplinary Graduate School of Science and Engineering
Tokyo Institute of Technology
Yokohama, Japan

KEY WORDS biological matrix · cesium · magnetic elimination · magnetic nanoparticles · Prussian blue · seawater

INTRODUCTION

Magnetic elimination systems that use functional nanoparticles represent a promising approach for the removal of hazardous carcinogenic substances such as contaminated radioactive chemicals from seawater.

Over the past year in Japan, large amounts of radioactive contaminants have leaked and spread over a large area from the disaster site at the Fukushima Daiichi nuclear power station. On March 11, 2011, the Great East Japan Earthquake hit (magnitude of 9.0) caused a huge tsunami wave which destroyed the power supply for the cooling system for the hot nuclear fuel rods. Ultimately, a serious meltdown of the overheated fuel rods caused the release of radioactive chemicals into the environment (1–4). In terms of long-terms effects, of the radioisotopes that were released, cesium–137 (^{137}Cs) and strontium–90 (^{90}St) have much longer half-lives than iodine–131 (^{131}I) (^{137}Cs: 30.2 years; ^{90}St: 28.9 years; ^{131}I: 8 days). Cesium displays a biological behavior profile similar to that of potassium; for example, cesium ions block potassium channels in the bio-membrane, and cesium accumulates in the muscle tissues of fish and animals, and is then transmitted through the food chain (5–9). Moreover, radioactive cesium is associated with carcinoma of the liver, kidney and bladder (10–12).

Prussian blue, a non-toxic blue pigment powder, has a crystal lattice structure, and is used as an antidote for the ingestion of radioactive cesium. Prussian blue exchanges its potassium ions for cesium ions, and thus has potential as a general cesium-eliminator (13–18). However, for Prussian blue to serve as an eliminator of cesium from a large amount of seawater, certain requirements are essential, including a precipitation tank having

considerable size and a long sedimentation time, a large-scale centrifugal separator, and an expensive filtration membrane. If, however, Prussian blue could be rapidly removed, it would greatly improve the procedure for eliminating radioactive cesium from seawater. Recently, we developed a novel form of magnetically guidable Prussian blue-coated nanocomposite clusters, termed "Prussian blueberry", which could help to overcome these obstacles and thus serve this urgent purpose.

Here, we report the preparation of Prussian blueberry through a layer-by-layer assembly method (19–21), and describe the morphology, structure, and physical properties of these nanoparticles. We also evaluate the ability of Prussian blueberry to eliminate cesium from seawater and biological matrices such as serum and milk.

MATERIALS AND METHODS

Preparation of PDDA-Coated Iron Oxide Nanoparticles

Initially, $FeCl_2$ (0.02 mol; Wako, Tokyo, Japan) and $FeCl_3$ (0.04 mol; Wako) were dissolved in 25 ml of distilled water (DW). When this solution was mixed with 25 ml of ammonium hydroxide (25%) in a 50 ml polypropylene tube under argon gas, a black magnetite slurry was precipitated. The slurry obtained was centrifuged at 3000 *g* for 10 min and washed 10 times with 35 ml of DW to remove ammonium chloride (22,23).

Subsequently, these magnetite nanoparticles were dispersed in DW to obtain 25 ml of magnetic fluid, and 0.01 M NaOH was added to adjust the pH to 9.0. Poly (diaryldimethylammonium chloride) (PDDA; 0.25 g) was mixed with DW to obtain 25 ml of aqueous PDDA solution, and 0.01 M NaOH was added to adjust the pH to 9.0. The magnetic fluid and the PDDA solution were then mixed and incubated for 2 h at room temperature. This mixture was then centrifuged at 9000*g* for 20 min and washed three times with 35 ml of DW to eliminate any excess PDDA; purified PDDA-coated iron oxide nanoparticles (PDDA@IO) were thus obtained.

Preparation of Prussian Blue

$FeCl_3$ (0.04 mol; Wako) was dissolved in 25 ml of DW in a 50 ml polypropylene tube. Potassium ferrocyanide (0.01 mol; Wako) was dissolved in 25 ml of DW, also in a 50 ml polypropylene tube. These solutions were then mixed and Prussian blue was obtained. Water-insoluble Prussian blue can be obtained from potassium ferrocyanide and an excess of $FeCl_3$. This Prussian blue slurry was centrifuged at 5000*g* for 15 min and washed five times with 35 ml of DW to eliminate excess $FeCl_3$.

Preparation of Prussian Blueberry

PDDA@IO (1 g) was dispersed in 10 ml of DW, and 0.01 M HCl was added to adjust the pH to 6.0. Prussian blue (3 g), the pH of which ranges from 2.4 to 2.7, was dispersed in 10 ml of DW to which 0.01 M NaOH was added to adjust the pH to 6.0. The slurry obtained was then mixed thoroughly at room temperature in a 50 ml polypropylene tube. DW (25 ml) was added to this mixture and a permanent magnet (1.4 tesla) was used to eliminate any excess Prussian blue from the Prussian blue-coated PDDA@IO. Prussian blue alone is not attracted by a magnetic field, and so we could magnetically separate the Prussian blueberry from the mixture of Prussian blueberry and non-magnetic Prussian blue. This purification step was repeated eight times to obtain and Prussian blueberry (Fig. 1).

Preparation of Simulated Seawater

Sodium chloride (26.5 g), magnesium chloride (3.26 g), magnesium sulfate (2.07 g), calcium sulfate (1.36 g) and potassium chloride (0.714 g) were dissolved in 966 ml of DW to obtain simulated seawater (24). Cesium chloride was then dissolved in this simulated seawater.

Determination of the Nanoparticle Size and Zeta Potential

The particle sizes and surface electrical charges (zeta potentials) of iron oxide, PDDA@IO, Prussian blue, and Prussian blueberry were analyzed with an electrophoretic light scattering spectrophotometer (ELS-8000 J; Otsuka Electronics, Osaka, Japan), as previously described (23). The nanoparticles were suspended in DW and the pH was adjusted by the addition of 0.01 M HCl or 0.01 M NaOH.

Transmission Electron Microscopy Using a Negative Staining Technique

The morphology of each nanoparticle and composite was characterized by use of negative staining with 1% uranyl acetate and transmission electron microscopy (TEM, JEOD JEM-2100) at an accelerating voltage of 200 kV, as previously described (22). To enhance the contrast of the morphological details at the molecular level, nanoparticles were surrounded with dense materials (25) such as uranyl acetate, ammonium molybdate, or sodium phosphotungstate.

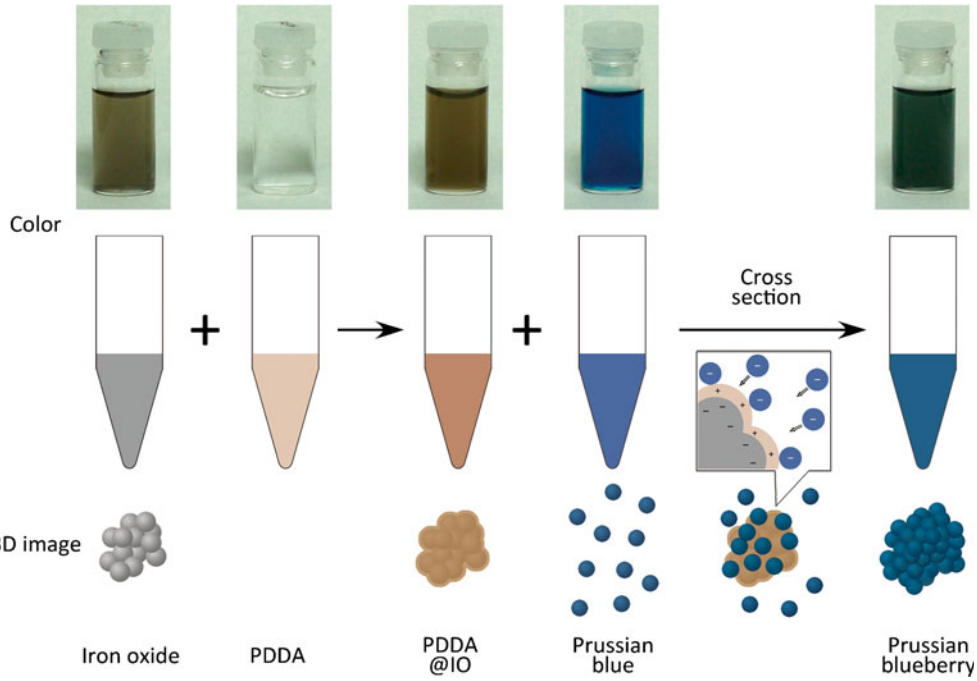

Fig. 1 Schematic representation of the Prussian blueberry-preparation.

X-Ray Diffraction Analysis

X-ray diffraction (XRD) analysis was performed to determine the crystalline phases of the samples, as described previously (26). XRD data were acquired by means of a coupled Theta: 2-Theta scan on a Rigaku Ultima-III diffractometer equipped with a copper x-ray tube, parafocusing optics, computer-controlled variable slits and a diffracted beam monochromator.

X-Ray Photoelectron Spectroscopy Analysis

X-ray photoelectron spectroscopy (XPS) analysis was performed to determine the surface composition and chemistry of the samples, as previously described (27). The analytical parameters were as follows: (1) instrument, PHI Quantum 2000; (2) X-ray source, monochromated Alkα 1486.6 eV; (3) acceptance angle, ±23°; (4) take-off angle, 45°; (5) analysis area, 1400 μm × 300 μm; and (6) charge correction, C1s 284.8 eV.

Fourier Transform Infrared Spectroscopy Analysis

Fourier transform infrared (FTIR) spectroscopy analysis was performed to provide specific information on the chemical bonding and molecular structure of the materials (28,29) by using an FTIR microscope (Nicoret 500 FT-IR, Thermo Fisher Scientific, MA) in the transmission mode and equipped with a variable angle Specular Reflectance Accessory (Specta Tech., USA).

Inductively Coupled Plasma Mass Spectrometry

The cesium concentration in the simulated seawater, serum, and milk was measured by using inductively coupled plasma mass spectrometry (ICP-MS: ICPM-8500, Shimadzu Corporation, Kyoto, Japan) according to the procedure described by Vanhoe *et al.* (30).

Magnetic Attraction Test

To test the magnetic attraction of Prussian blueberry, we used a 96-well magnetic ring plate (Fig. 2; Ambion, Austin, TX), which generated a doughnut-shaped magnetic gradient. The intensity of the magnetism at the ring of the plate was found using a Teslameter (GM-5005, Denshijiki Industry Co.,Ltd, Tokyo, Japan) to be 0.42 tesla. This plate was attached under a 96-well microtiter plate, and the degree of magnetic attraction of the nanoparticles was then recorded by using a digital camera.

RESULTS

Optimal Conditions for the Preparation of Prussian Blueberry

Initially, we modified the surface of the iron oxide nanoparticles with the cationic polymer PDDA. To determine the optimal conditions for PDDA-modification, we measured the zeta potential of the iron oxide nanoparticles

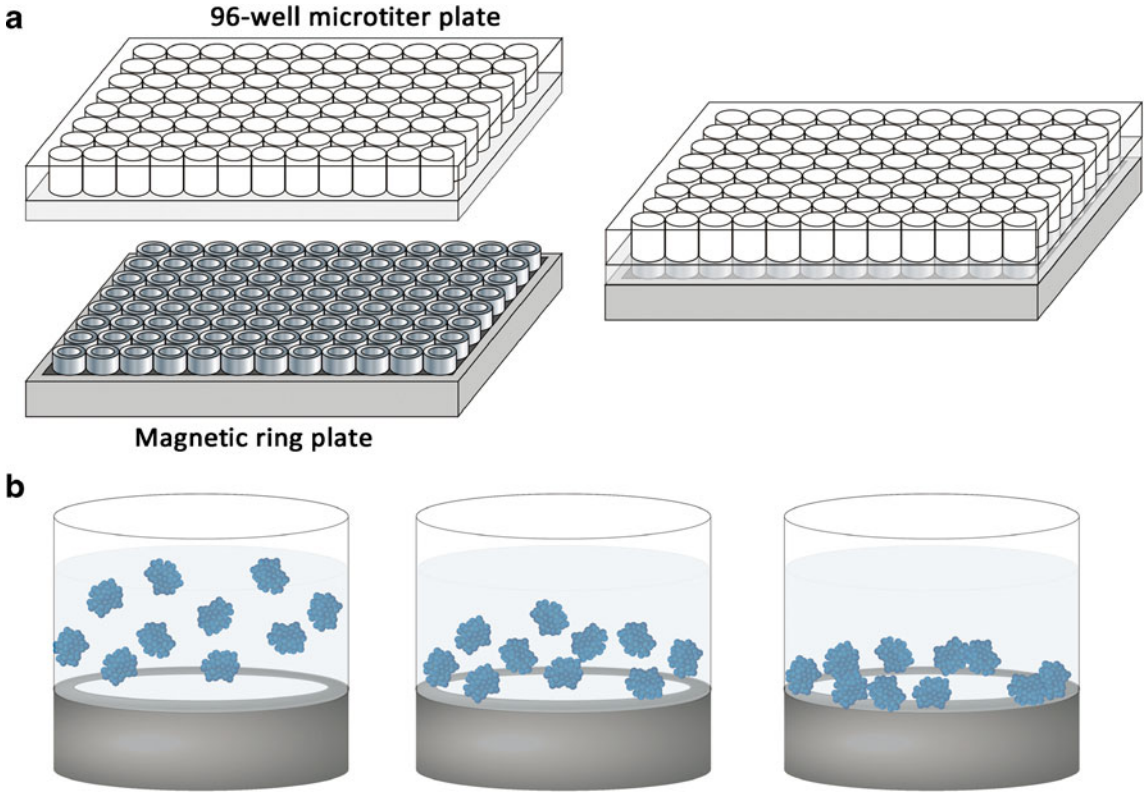

Fig. 2 Schematic representation of the 96-well ring plate-associated magnetic attraction of Prussian blueberry. (**a**) Magnetic attraction of Prussian blueberry was observed by using a magnetic plate to generate a ring-shaped magnetic field gradient. (**b**) Diagrammatic representation of the magnetically attracted Prussian blueberry on magnetic ring.

and PDDA@IO at pH 4–10 (Fig. 3). We found that the difference in the zeta potential between these nanoparticles was maximal at pH 9.0 within the range of conditions tested (iron oxide nanoparticles: –17.3 mV; PDDA@IO: 33.0 mV). We therefore coated the surface of the iron oxide nanoparticles with PDDA at this optimal value of pH 9.0. We then compared the zeta potential of PDDA@IO and Prussian blue over the same pH range and found that the nanoparticles exhibited a maximal difference in zeta potential at pH 6.0 (PDDA@IO: 39.9 mV; Prussian blue: −36.1 mV). It was decided to coat the PDDA@IO with Prussian blue at pH 6.0. Subsequently, the electrostatic force between the anionic Prussian blue and the cationic PDDA@IO formed Prussian blueberry through a layer-by-layer mechanism. These data suggest that the Prussian blueberry are composed largely of negatively charged Prussian blue with a smaller amount of positively charged PDDA@IO, and that the surface area of the positively-charged PDDA@IO nanoparticles is entirely covered with negatively-charged Prussian blue. The average particle sizes of the iron oxide, PDDA@IO, Prussian blue, and Prussian blueberry were 337.9 nm (pH=9.0), 161.4 nm (pH=9.0), 171.0 nm (pH=6.0), and 304.2 nm (pH=6.0), respectively (Fig. 3).

Morphological and Physiological Properties of Prussian Blueberry

We evaluated the formation of the nanoparticles by using negative staining and transmission electron microscopy (Fig. 4). The electron micrographs revealed that Prussian blueberry had a form resembling that of a mulberry and were composed of peripheral, negatively-charged Prussian blue surrounding positively-charged PDDA@IO. These results are consistent with the zeta potential of Prussian blueberry, as shown in Fig. 3. Subsequently, we used XRD to examine the crystal structure of Prussian blueberry (Fig. 5) and found that the data for iron oxide and PDDA@IO were nearly identical. This result implies that either the amount of PDDA was beneath the level of XRD detection or that the coating on the Fe_3O_4 particles was too thin to contribute to the diffraction scan. We confirmed that the Prussian blueberry contained both Fe_3O_4 and Prussian blue by using the ICDD/ICSD powder diffraction database. We also investigated the surface conditions of the Prussian blueberry, Prussian blue, PDDA@IO and iron oxide by using XPS (Fig. 6). The C1 peak (284 eV) and N1 peak (397 eV) suggested the existence of –CN groups associated with the [Fe^{II}–CN–Fe^{III}] of Prussian

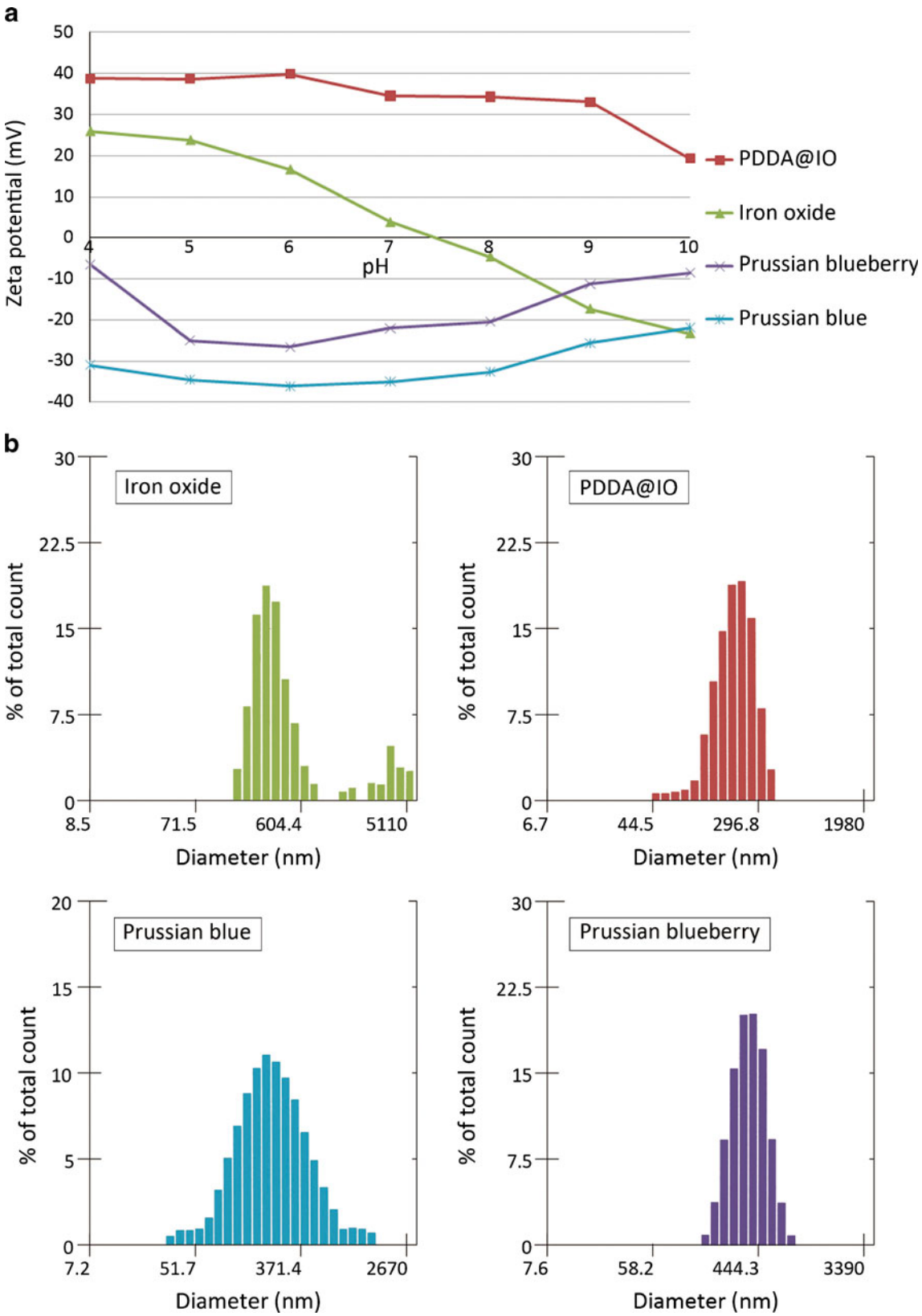

Fig. 3 (**a**) Surface electrical charges of nanoparticles and nanocomposite particles at different pH values. (**b**) Size-distribution of nanoparticles.

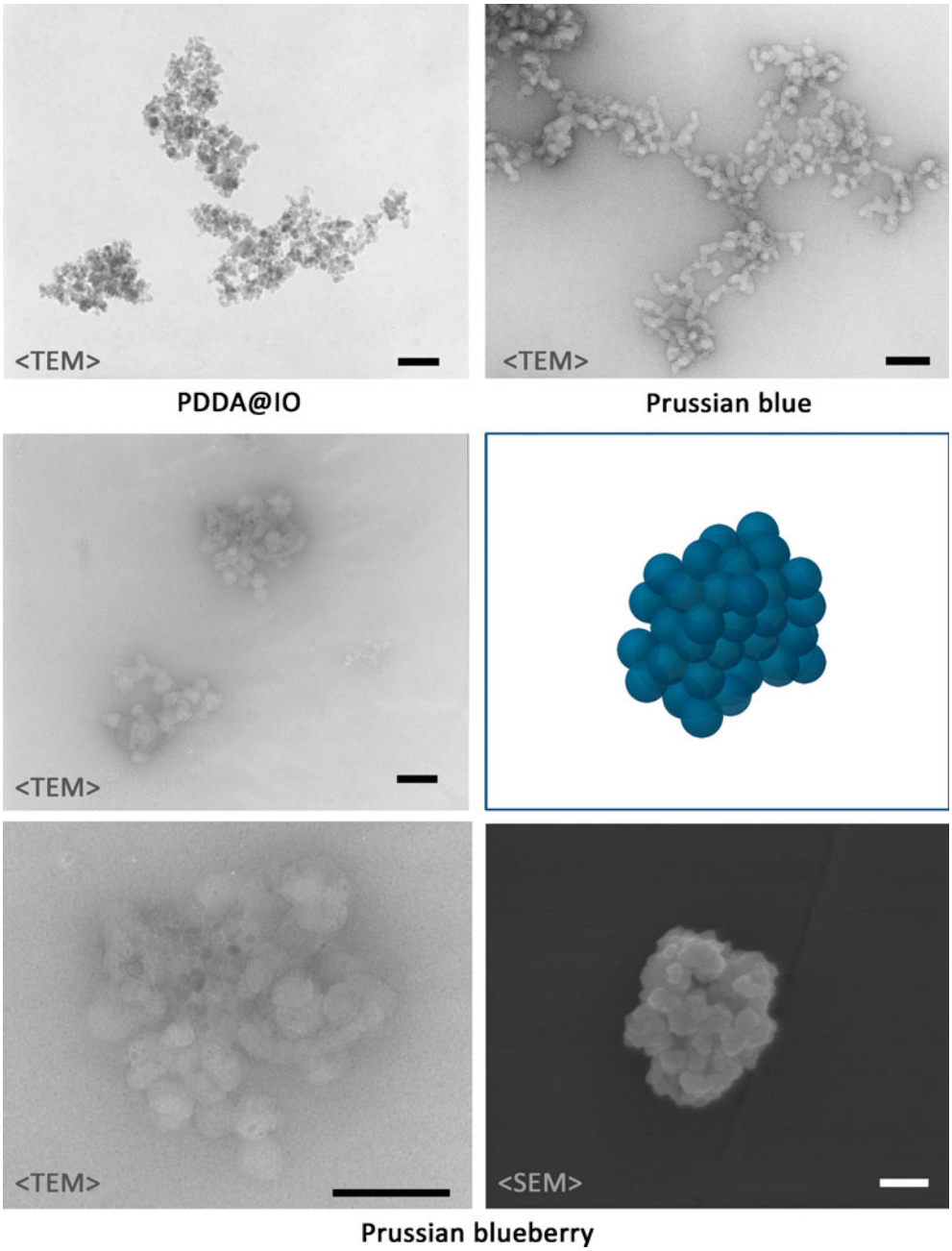

Fig. 4 Electron micrographs of Prussian blueberry and the source materials. Bar, 100 nm.

blue. The first peak (709 eV) and the second peak (711 eV) of Fe2p3 originated from iron oxide and iron cyanide, respectively. The FTIR spectra of the materials were compared (Fig. 7). Bands at ~3379 and 1614 cm^{-1}, as well as additional bands outside the wavelength range (< 650 cm^{-1}) suggested the existence of Fe_3O_4. A band at 1472 cm^{-1} indicated the existence of PDDA in the PDDA@IO nanocomposites. Prussian blue had an intense band at ~2076 cm^{-1}, which was identical to its library reference spectrum. This spectrum was not altered when the Prussian blue had combined with PDDA@IO. Prussian blue and Prussian blueberry contained an additional OH (hydroxyl) species (a band at ~3635 cm^{-1}). Finally, magnetic characterization was performed using a vibration sample magnetometer by applying a maximum field of 5 KOe (Fig. 8). Iron oxide, PDDA@IO, and Prussian blueberry exhibited a saturation magnetization of 49.9, 49.6, and 28.8 emu/g, respectively, and almost no coercive force, whereas Prussian blue exhibited almost no magnetism.

Taken together, these data reveal that the positively charged surface of PDDA@IO nanoparticles is coated with negatively charged Prussian blue. Prussian blueberry displayed superparamagnetism originating from their iron oxide core. Accordingly, we hypothesized that these

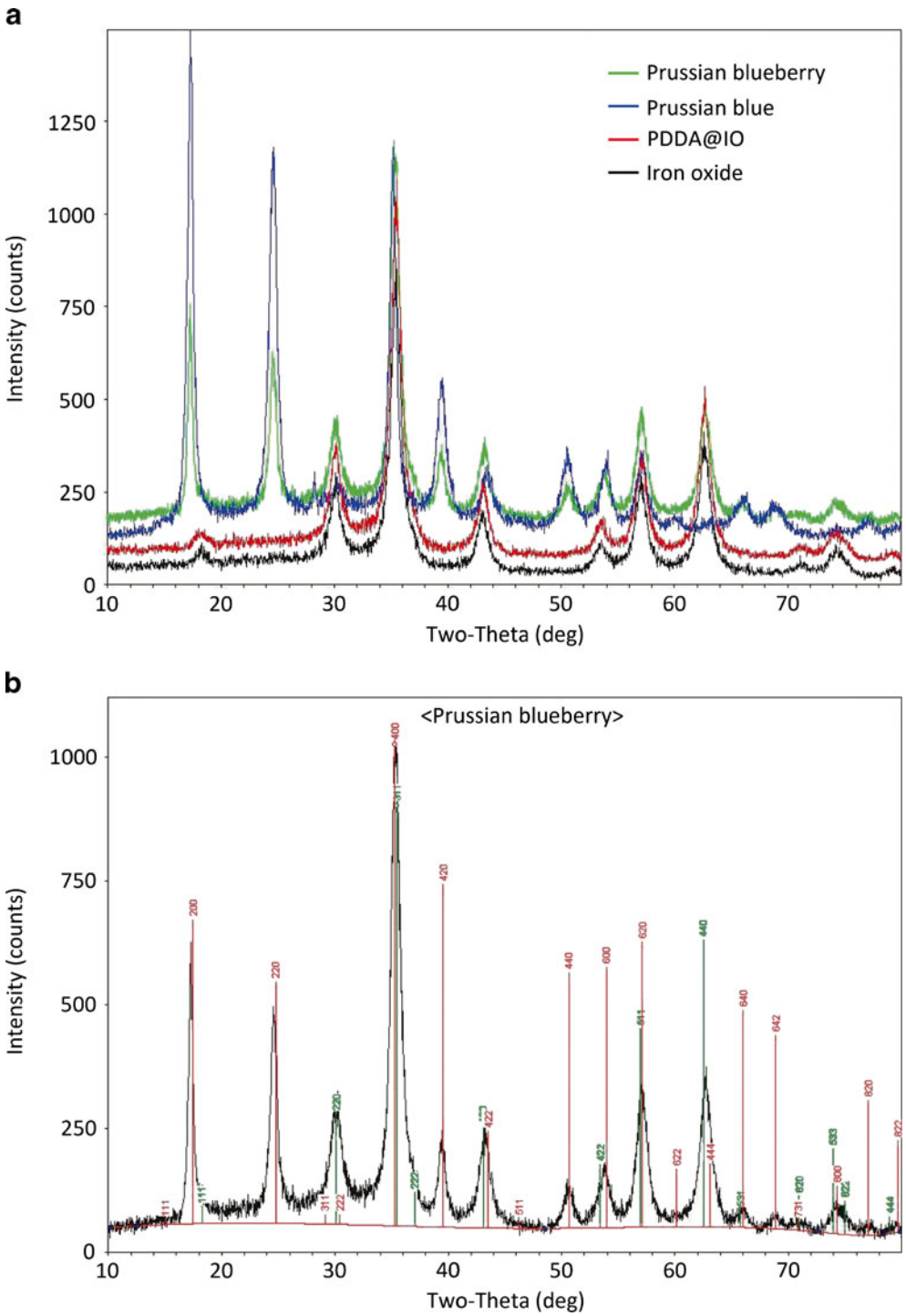

Fig. 5 XRD peaks of Prussian blueberry and source materials. (**a**) Overlay of data from all four samples with y-scale offset for clarity. (**b**) Best matches obtained by comparing background-subtracted raw data with ICDD (http://www.icdd.com/translation/pdf2.htm)/ICSD (http://www.fiz-karlsruhe.de/icsd_web_output_mngt_powder_pat.html?&L=11) powder diffraction database data for Prussian blueberry. *Red*, Prussian blue; *green*, Fe_3O_4.

characteristics would be suitable for the magnetically controlled elimination of cesium from seawater.

Stability of Prussian Blueberry at Different pH Levels

We investigated the stability of Prussian blueberry in seawater at various pH levels (Fig. 9). Five micrograms of nanocomposite particles were dispersed in 250 µl of seawater at pH 2–13, and each sample was introduced into a 96-well plate. After vigorous agitation using a plate mixer, a ring-shaped magnetic gradient was generated at the bottom of the culture plate. At pH 2–10, the fluid color remained blue, and blue-colored magnetic nanoparticles accumulated in a ring shape. At pH 11–13, however, the color of the magnetic nanoparticles changed from blue to

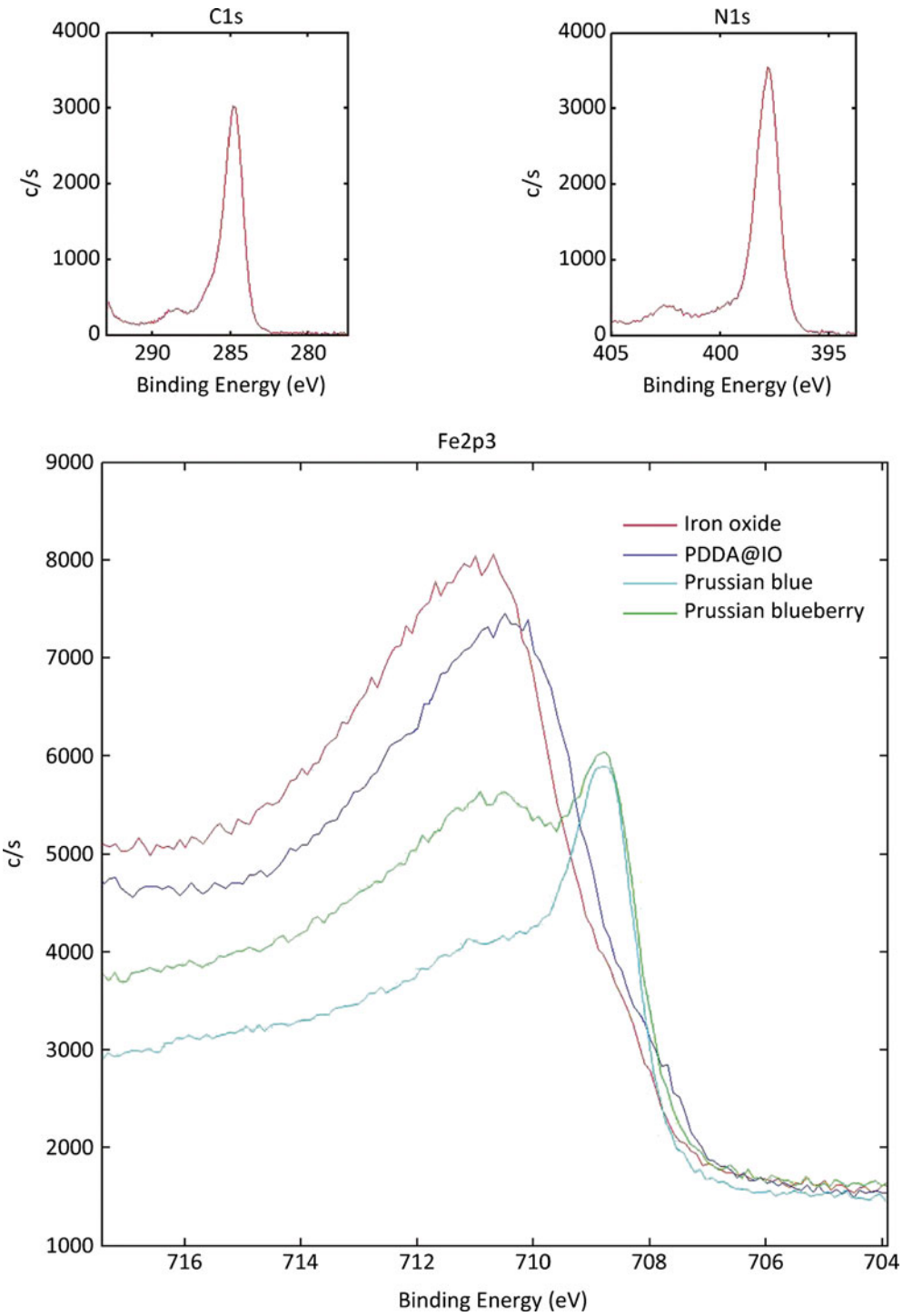

Fig. 6 XPS profiles of Prussian blueberry.

light brown, and it became difficult to attract them magnetically.

Magnetic Elimination of Cesium by Prussian Blueberry

We then examined the degree of magnetic cesium-elimination that could be achieved by using Prussian blueberry. We prepared seawater (3 ml) containing cesium (150 ppm) and mixed it with Prussian blueberry (5 mg). This mixture was passed through a sintered stainless steel filter under a magnetic field (0.56 tesla). A stainless filter combined with magnets creates much more powerful magnetic field gradients close to magnetic stainless steel (SUS430) granules (27) or magnetic stainless steel wool (31) than when magnets alone are used. The pore size of the

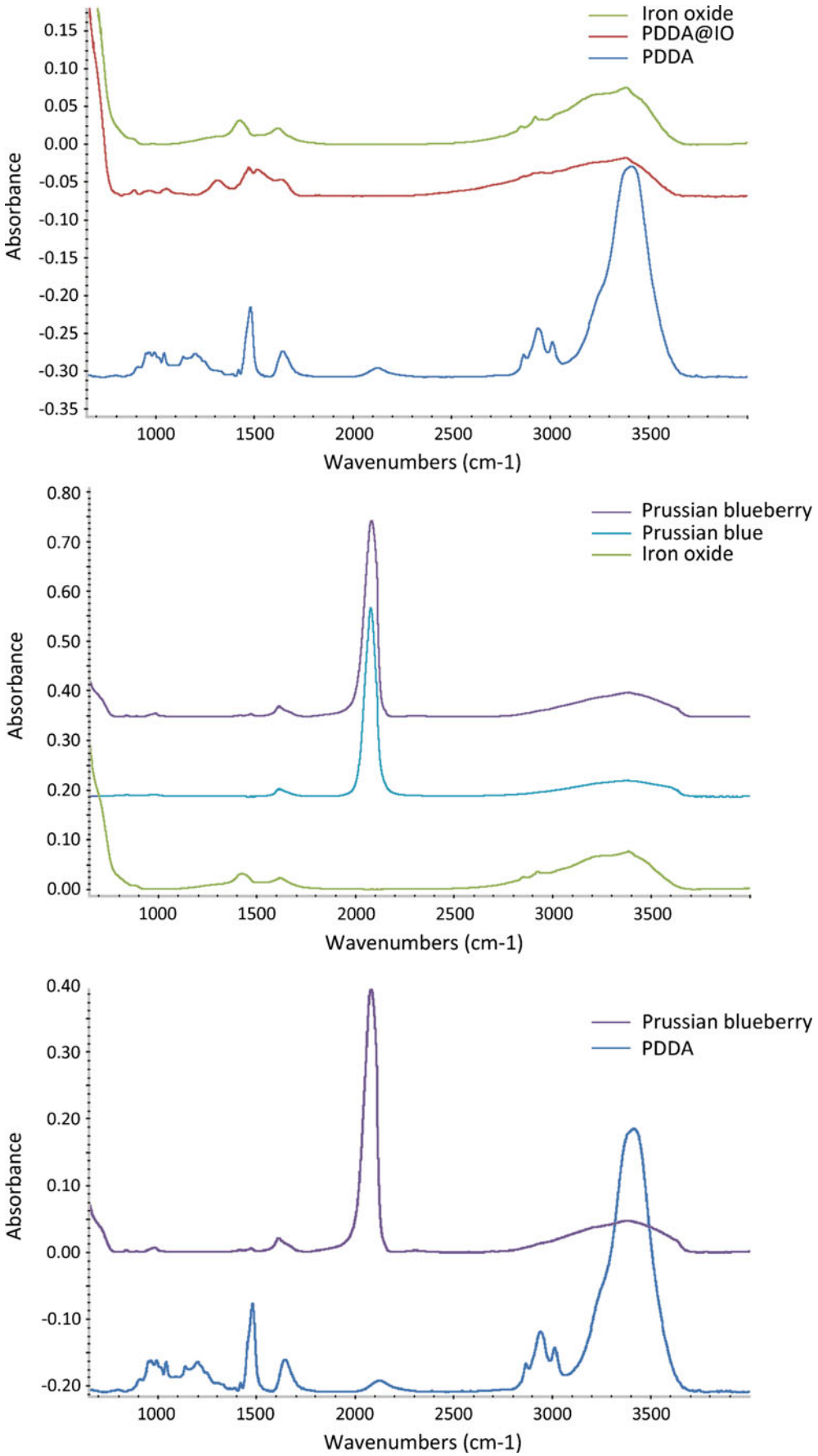

Fig. 7 FTIR spectra of Prussian blueberry and the source materials.

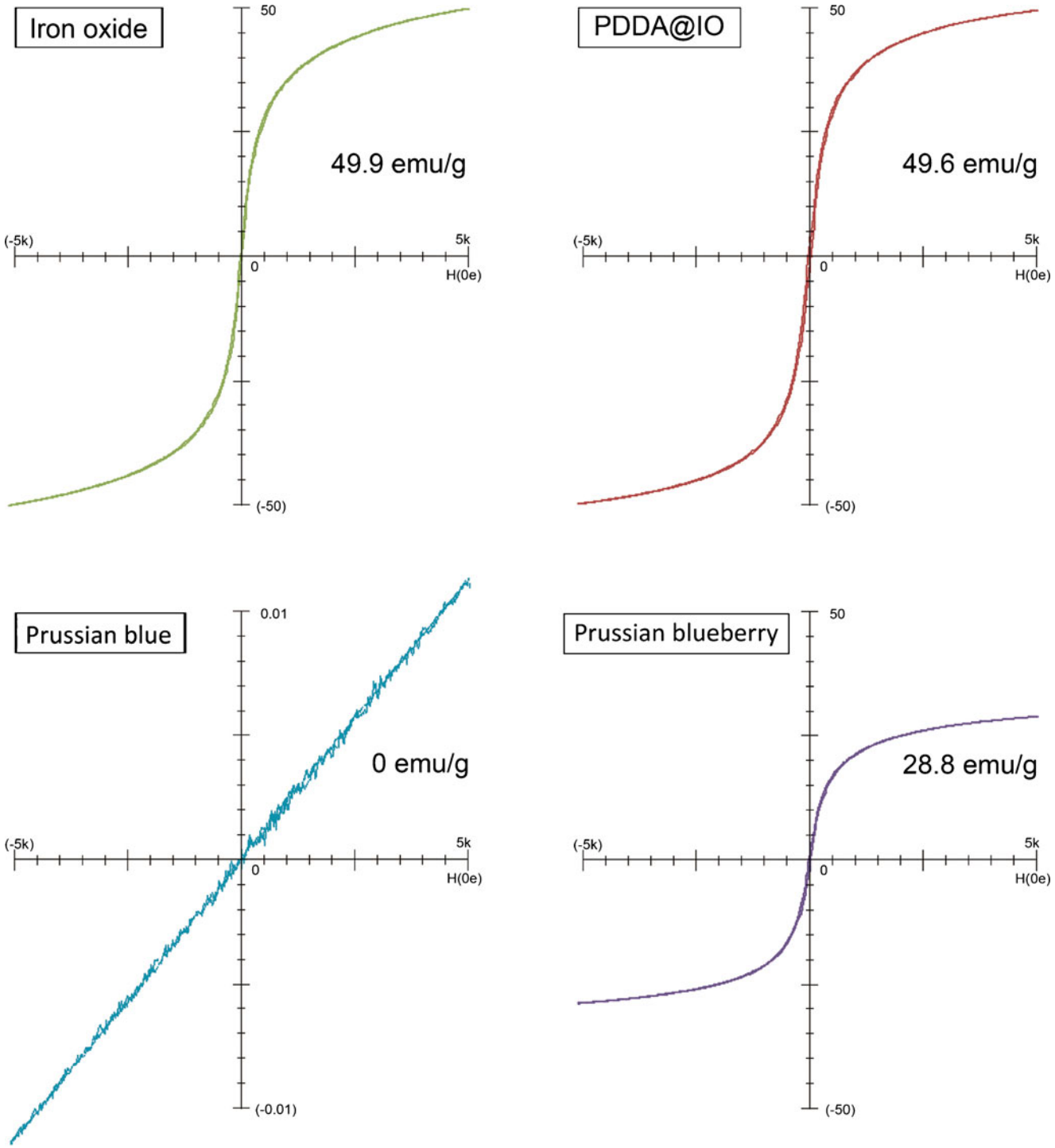

Fig. 8 Magnetization curves of Prussian blueberry and source materials.

sintered stainless steel filter was much larger than the size of the nanoparticles, and therefore, magnetic nanoparticles such as Prussian blueberry could pass through this filter in the absence of a magnetic field (Fig. 10). The cesium concentration of the filter-treated seawater was measured. At pH 4.5, 7.0, and 9.5, Prussian blueberry eliminated similar amounts of cesium from the seawater. Under a magnetic field for less than 15 sec, the cesium concentration was decreased to 34.2%–34.8% of the non-treatment groups at pH 4.5 to 9.5. The degree of cesium-elimination was 84.7% to 86.7% of that achieved with the centrifuged Prussian blue group. Centrifugation was

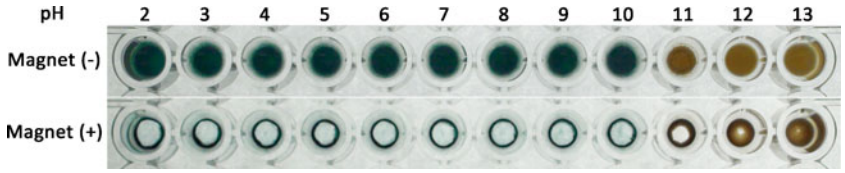

Fig. 9 Magnetic attraction and stability of Prussian blueberry dispersed in simulated seawater at different pH values.

required to eliminate the Prussian blue because Prussian blue cannot be accumulated magnetically.

Large-Scale Study of the Magnetic Elimination of Cesium from Seawater Under Agitation

We tested the practical applicability of using Prussian blueberry for cesium-elimination from a larger volume of seawater than that described above (3 mL) and under agitation, similar to that of an ocean wave. Specifically, we prepared 150 ml of seawater containing cesium (150 ppm) and mixed it with Prussian blueberry (250 mg). A magnetic bar (1.0 tesla; Niroku Seisakujo, Kobe, Japan) was introduced into this mixture. When the nanoparticles accumulated at the magnetic bar, an agitation force was generated by using a wave mixer at 40% of the maximum rotations per minute and 40% of the maxim amplitude (WEB-30; AS ONE, Osaka, Japan). The cesium concentration in the magnetic bar-treated seawater was measured by using ICP-MS in a similar manner, as shown in Fig. 10. At pH 4.5, 7.0, and 9.5, Prussian blueberry eliminated similar amounts of cesium from the seawater. Under a magnetic field for 5 min, the cesium concentration was decreased to 35.0% to 35.6% of that in the non-treatment groups (Fig. 11).

Magnetic Elimination of Cesium from Biological Matrices

We also evaluated the degree to which Prussian blueberry could induce magnetic cesium-elimination from biological matrices such as serum and milk. We prepared fetal bovine serum (45 ml) and cow's milk (45 ml) containing cesium chloride (150 ppm) and mixed each of them with Prussian blueberry (75 mg) in 50 ml polypropylene tubes. After the 15-min incubation at room temperature, each tube was attached to a magnet that had an outer yoke (Hinode Pipe, Tokyo, Japan) (22). The cesium concentration was measured by using ICP-MS as shown in Fig. 10. Under a magnetic field for 5 min, the cesium concentration of the serum and milk was decreased to 32.5% and 30.5% of that in the non-treatment groups, respectively (Fig 12).

DISCUSSION

This study represents the first demonstration that Prussian blue-coated magnetic nanoparticles prepared through a layer-by-layer procedure (19–21) can efficiently capture cesium from seawater, serum, and milk, and that the cesium-captured nanoparticles can be rapidly removed by the application of a magnetic gradient field.

Prussian blue, also known as ferric (III) hexacyanoferrate (II), has the empirical formula of $Fe_4[Fe(CN)_6]_3$ and is a highly active ion-exchanger with a strong affinity for cesium and thallium (13–18). In terms of safety, Prussian blue is known to be a nontoxic polymeric cyanometalate, because its cyanide groups are tightly bound to Fe. Radiogardase^{TM} (32,33), a Prussian blue powder mixed with microcrystalline cellulose in gelatin capsules, is used to treat patients contaminated with radioactive cesium or thallium (http://www.heyltex.com/radiogardasePackageInsert.php). Prussian blue can also be used to treat wastewater contaminated with radioactive cesium, but the treatment of a large amount of wastewater with Prussian blue is impractical due to the requirements of a precipitation tank, centrifugal separators, and membrane filters.

We hypothesized that if sufficient Prussian blue could be attracted by a magnetic field, it would be possible to rapidly and effectively remove cesium-captured Prussian blue from wastewater. Prussian blue itself has almost no magnetism and cannot be attracted with a neodymium magnet (34); therefore, we developed Prussian blue-coated magnetic nanoparticles with the capacity to efficiently remove cesium from seawater when we applied a magnetic gradient field.

Prussian blue-coated iron oxide nanoparticles have very recently been developed as peroxidase-like catalysts (35,36), because iron oxide has intrinsic peroxidase activity and Prussian blue catalyzes the reduction of hydrogen peroxidase. However, these nanoparticles are of a much smaller diameter than Prussian blueberry (35), and therefore necessitate a much longer time for the magnetic accumulation to be carried out. Moreover, a much larger amount of source material would also be needed, because most of the iron oxide nanoparticles are changed to Fe^{3+} during preparation, such that the surface of only a few iron oxide nanoparticles are coated with Prussian blue (36). These properties of classic Prussian blue-coated iron oxide nanoparticles make them

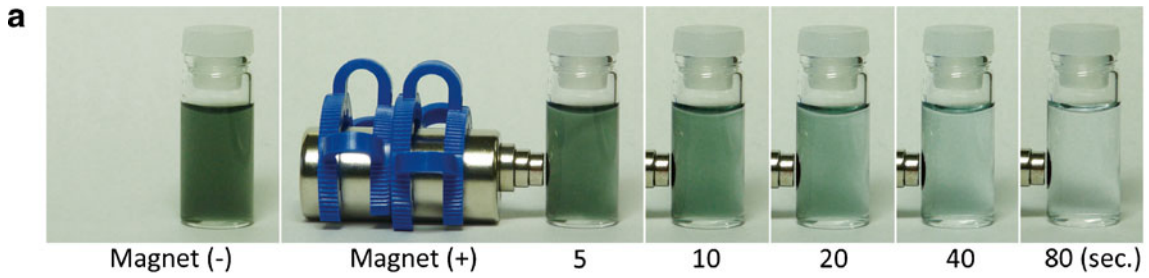
a
Magnet (-)
Magnet (+)
5
10
20
40
80 (sec.)

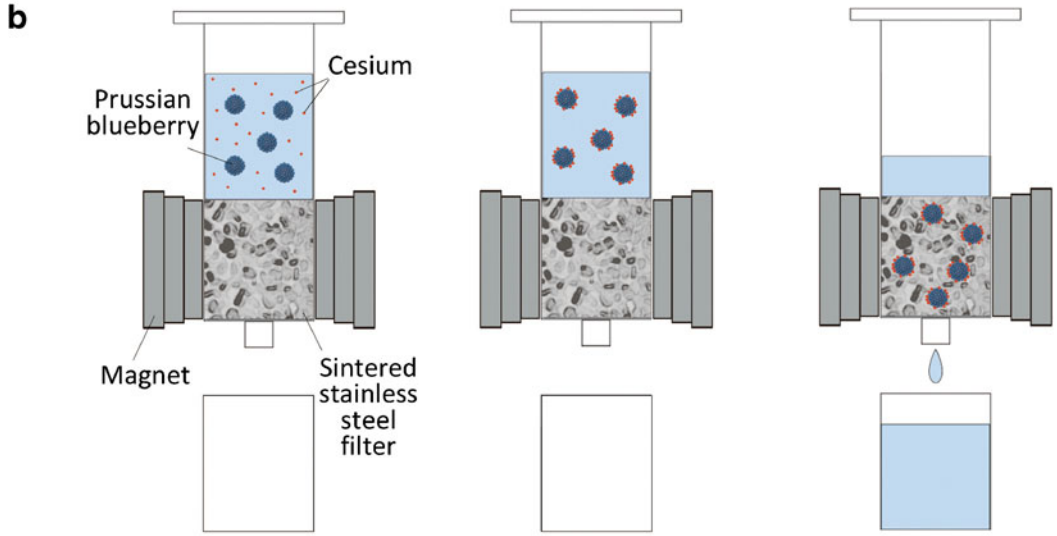
b
Cesium
Prussian blueberry
Magnet
Sintered stainless steel filter

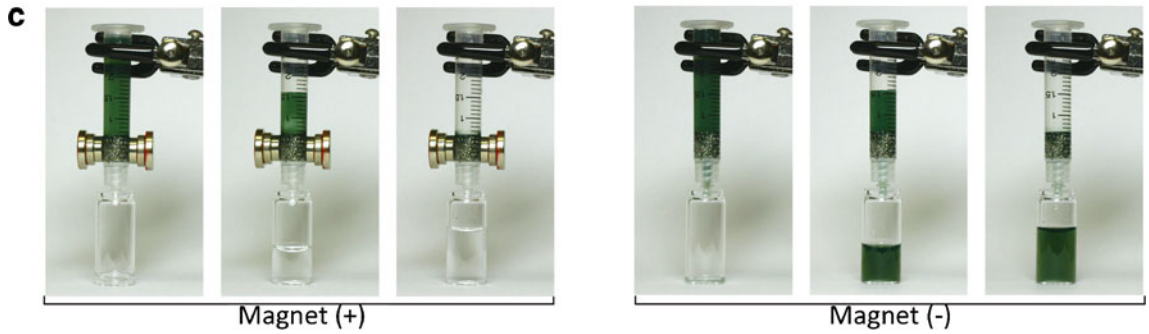
c
Magnet (+)
Magnet (-)

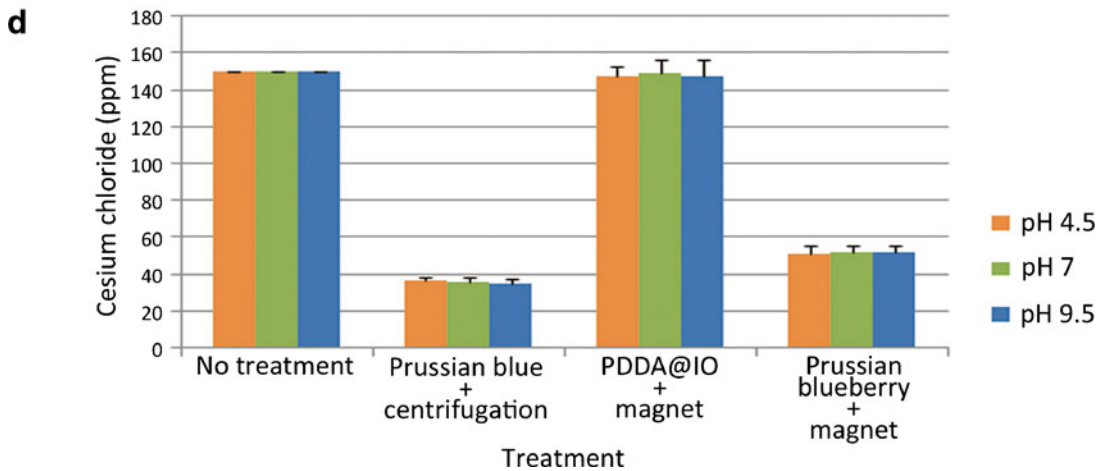
d
Cesium chloride (ppm)
180
160
140
120
100
80
60
40
20
0
No treatment
Prussian blue + centrifugation
PDDA@IO + magnet
Prussian blueberry + magnet
Treatment
pH 4.5
pH 7
pH 9.5

◀ **Fig. 10** Magnetic elimination of cesium chloride from simulated seawater by Prussian blueberry. (**a**) Prussian blueberry (3 mg) was mixed with artificially made seawater and a neodymium magnet (0.64 tesla) was attached to the side of the vial. The degree of magnetic attraction of Prussian blueberry was recorded by using a digital camera. (**b**, **c**) Diagram (**b**) and photograph (**c**) of sintered stainless granule filter for eliminating cesium captured by Prussian blueberry. (**d**) Each nanoparticle (5 mg) was mixed with cesium dissolved in seawater. The Prussian blue group was centrifuged at 15,000*g* for 3 min and the cesium concentration of the supernatant was measured.

unsuitable for efficient magnetically guided cesium elimination. Meanwhile, calixarene derivative-coated magnetic nanoparticles have been reported to be applicable to the magnetic elimination of cesium (37), but these calixarene-derived nanoparticles are much more expensive than Prussian blue and PDDA. Therefore, the treatment of a large amount of radioactive cesium-contaminated water using these nanoparticles is not feasible.

To overcome these drawbacks, we devised Prussian blueberry as an easier and less expensive preparation of cesium-removing magnetic nanoparticles. We confirmed that Prussian blueberry have practical application to the rapid elimination of cesium from seawater (Figs. 10, 11), fetal bovine serum, and cow's milk (Fig. 12) within a period of 5 min. In addition to the treatment of waste seawater, our results suggest that Prussian blueberry may have further applications, including in cases requiring immediate treatment, such as blood purification of cesium-contaminated patients or as a prophylactic in cases of radioactive cesium ingestion from breast milk or dairy foods (38).

In terms of the safety of conventional Prussian blue compared with that of the type used here, if radioactive cesium-trapped Prussian blue were to spread out in the environment, there is the potential for serious secondary radioactive contamination, because there is currently no procedure for the specific removal of Prussian blue.

In the near future, the combination of Prussian blueberry, a superconducting magnet, and a magnetic filter will accomplish the rapid elimination of cesium even from large amounts of water contaminated with

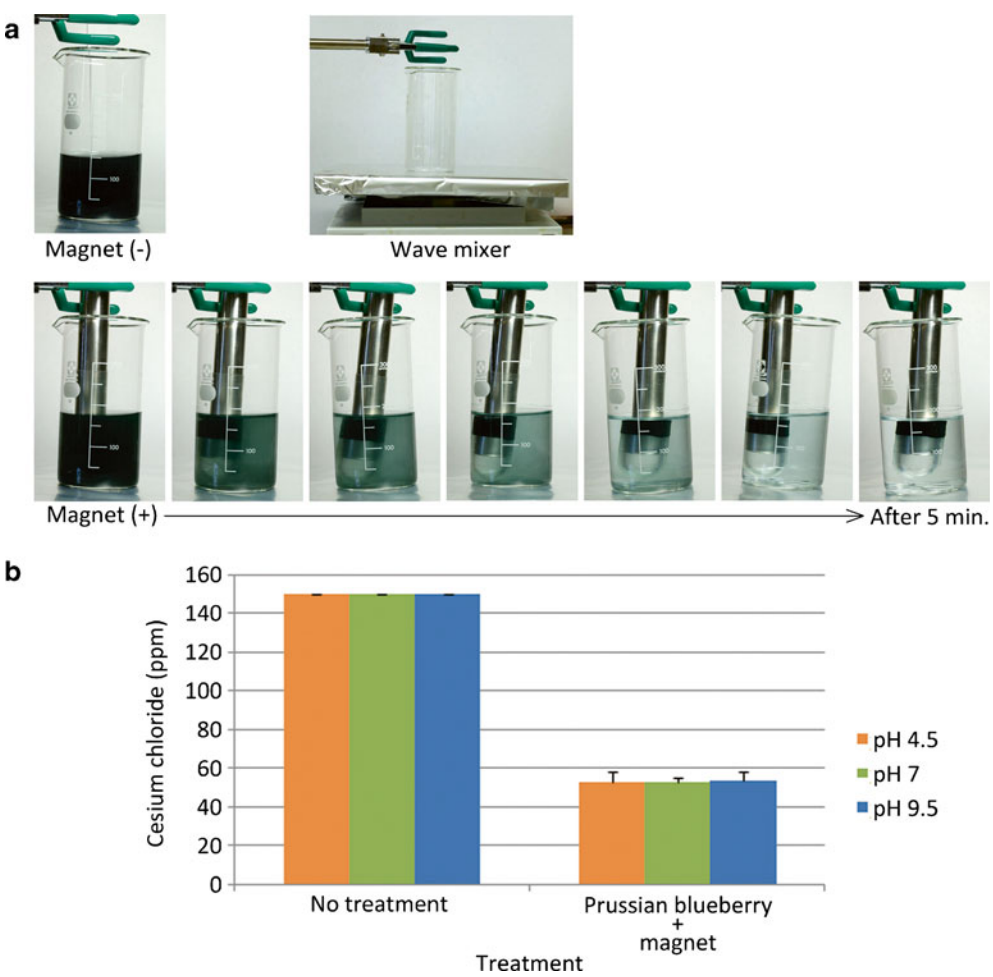

Fig. 11 Magnetic elimination of cesium chloride from a large volume of simulated seawater under agitation by Prussian blueberry.

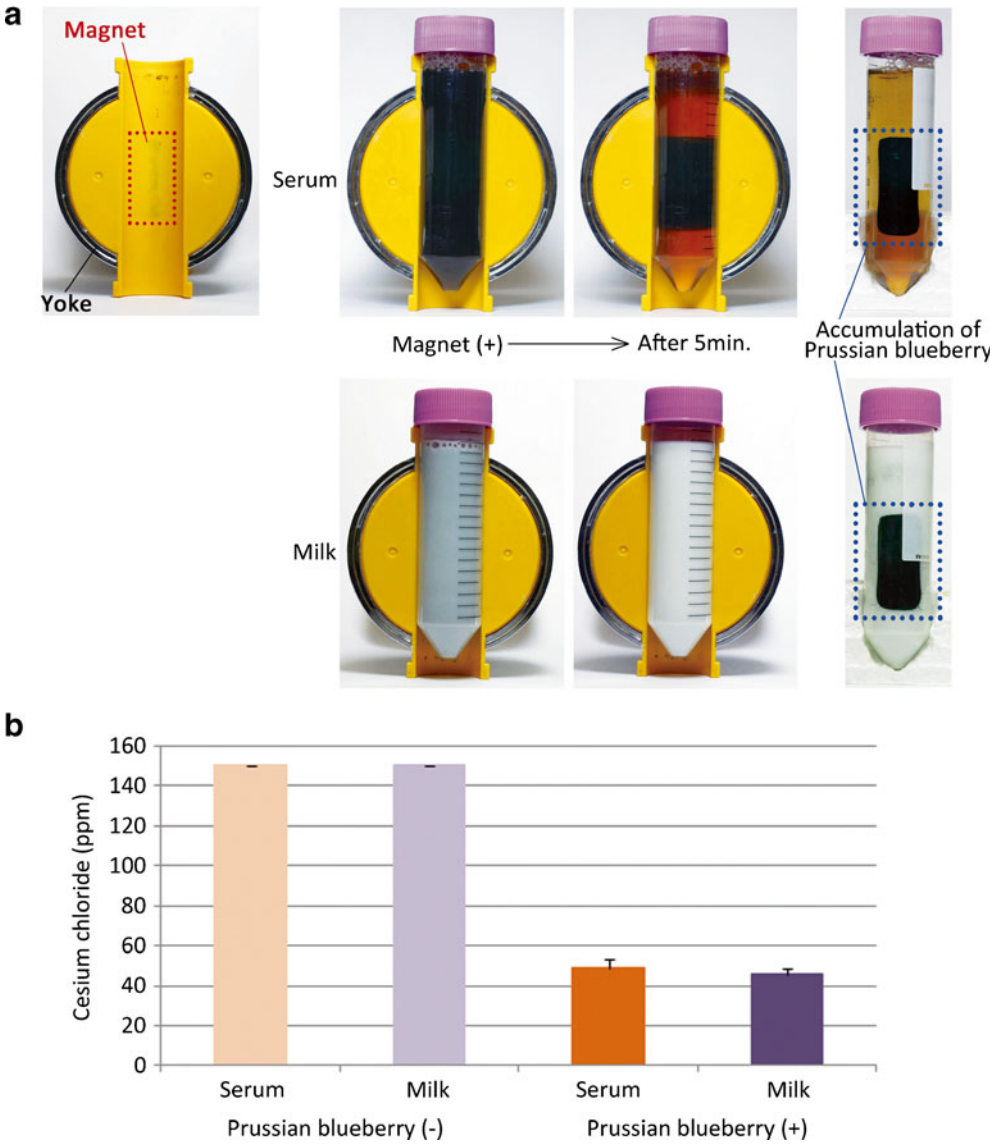

Fig. 12 Magnetic elimination of cesium chloride from serum and milk by Prussian blueberry.

radioactivity. The intensity of the magnetic field of a superconducting magnet is generally over 20 times greater than that of a neodymium magnet, and a magnetic filter can sharply enhance its magnetic field gradient. This combination is also advantageous in terms of reducing the size of a purification system needed because it requires much less space than the current purification systems that use precipitation tanks. Moreover, even at the domestic level, the combination of the Prussian blueberry, a neodymium magnet, and a magnetic filter could easily and rapidly remove radioactive cesium from drinking water, tea, cow's milk, mother's milk, *etc*. Prussian blueberry will likely have an important role in the prevention of radioactive cesium-induced cancer (10–12).

In summary, a procedure for the preparation of Prussian blueberry under optimal conditions is reported. These nanoparticles were used to achieve the rapid magnetic elimination of cesium from seawater and from biological matrices, such as serum and milk.

ACKNOWLEDGMENTS & DISCLOSURES

We dedicate this work to the late T. Terada, the late K. Nariai, and the many people who suffered in the March 11 disaster. We would like to acknowledge the staff of our respective institutes for their assistance. This work was supported by a Funding Program for the Next Generation of World-Leading Researchers (LS114) from the JSPS and by an Industrial Technology Research Grant (08C46049a) from the NEDO of Japan. The authors also wish to thank Mr. C.W.P. Reynolds, associated with the Department of International Medical Communications of Tokyo Medical University, for his careful and detailed assistance with the English of this paper.

REFERENCES

1. Leon JD, Jaffe DA, Kaspar J, Knecht A, Miller ML, Robertson RG, *et al.* Arrival time and magnitude of airborne fission products from the Fukushima, Japan, reactor incident as measured in Seattle, WA, USA. J. Environ. Radioact. 2011 (in press).
2. Pittauerová D, Hettwig B, Fischer HW. Fukushima fallout in Northwest German environmental media. J Environ Radioact 2011 (in press).
3. Lozano RL, Hernández-Ceballos MA, Adame JA, Casas-Ruíz M, Sorribas M, Miguel EG, *et al.* Radioactive impact of Fukushima accident on the Iberian Peninsula: Evolution and plume previous pathway. Environ Int 2011 (in press).
4. Manolopoulou M, Vagena E, Stoulos S, Ioannidou A, Papastefanou C. Radioiodine and radiocesium in Thessaloniki, Northern Greece due to the Fukushima nuclear accident. J Environ Radioact. 2011;102:796–7.
5. Davis JJ, Foster RF. Bioaccumulation of radioisotopes through aquatic food chains. Ecology. 1958;39:530–5.
6. Morgan F. The uptake of radioactivity by fish and shellfish I. Caesium-134 by whole animals. J Mar Biol Ass UK. 1964;44:259–71.
7. Kawamatsu F, Ishikawa Y. Natural variation of radionuclide 137Cs concentration in marine organisms with special reference to the effect of food habits and trophic level. Mar Ecol Prog Ser. 1997;160:109–20.
8. Duff MC, Ramsey ML. Accumulation of radiocesium by mushrooms in the environment: a literature review. J Environ Radioact. 2008;99:912–32.
9. Koulikov AO, Meili M. Modeling the dynamics of fish contamination by Chernobyl radiocaesium: an analytical solution based on potassium mass balance. J Environ Radioact. 2003;66:309–26.
10. Hahn FF, Muggenburg BA, Boecker BB. Hepatic neoplasms from internally deposited 144CeCl3. Toxicol Pathol. 1996;24:281–9.
11. Romanenko A, Morimura K, Wanibuchi H, Salim EI, Kinoshita A, Kaneko M, *et al.* Increased oxidative stress with gene alteration in urinary bladder urothelium after the Chernobyl accident. Int J Cancer. 2000;86:790–8.
12. Romanenko A, Morell-Quadreny L, Nepomnyaschy V, Vozianov A, Llombart-Bosch A. Pathology and proliferative activity of renal-cell carcinomas (RCCS) and renal oncocytomas in patients with different radiation exposure after the Chernobyl accident in Ukraine. Int J Cancer. 2000;87:880–3.
13. Thompson DF, Church CO. Prussian blue for treatment of radiocesium poisoning. Pharmacotherapy. 2001;21:1364–7.
14. Farina R, Brandão-Mello CE, Oliveira AR. Medical aspects of 137Cs decorporation: the Goiânia radiological accident. Health Phys. 1991;60:63–6.
15. Pearce J, Unsworth EF, McMurray CH, Moss BW, Logan E, Rice D, *et al.* The effects of Prussian blue provided by indwelling rumen boli on the tissue retention of dietary radiocaesium by sheep. Sci Total Environ. 1989;85:349–55.
16. Unsworth EF, Pearce J, McMurray CH, Moss BW, Gordon FJ, Rice D. Investigations of the use of clay minerals and Prussian blue in reducing the transfer of dietary radiocaesium to milk. Sci Total Environ. 1989;85:339–47.
17. Kargacin B, Kostial K. Reduction of 85Sr, 137Cs, 131I and 141Ce retention in rats by simultaneous oral administration of calcium alginate, ferrihexacyanoferrate(II), KI and Zn-DTPA. Health Phys. 1985;49:859–64.
18. Stather JW. Influence of Prussian blue on metabolism of 137 Cs and 86 Rb in rats. Health Phys. 1972;22:1–8.
19. Tedeschi C, Möhwald H, Kirstein S. Polarity of layer-by-layer deposited polyelectrolyte films as determined by pyrene fluorescence. J Am Chem Soc. 2001;123:954–60.
20. Yoon HC, Kim HS. Multilayered assembly of dendrimers with enzymes on gold: thickness-controlled biosensing interface. Anal Chem. 2000;72:922–6.
21. Rao SV, Anderson KW, Bachas LG. Controlled layer-by-layer immobilization of horseradish peroxidase. Biotechnol Bioeng. 1999;65:389–96.
22. Namiki Y, Namiki T, Yoshida H, Ishii Y, Tsubota A, Koido S, *et al.* A novel magnetic crystal-lipid nanostructure for magnetically guided *in vivo* gene delivery. Nat Nanotechnol. 2009;4:598–606.
23. Namiki Y, Fuchigami T, Tada N, Kawamura R, Matsunuma S, Kitamoto Y, *et al.* Nanomedicine for cancer: Lipid-based nanostructures for drug delivery and monitoring. Accounts Chem Res. 2011;44:1080–93.
24. Herring A. Japanese Salt and Foreign Salt. In: Herring A, editor. Tobacco & salt museum. Japan: Tobacco and Salt Museum; 2010. p. 67–95.
25. Woodcock CL, Woodcock H, Horowitz RA. Ultrastructure of chromatin: negative staining of isolated fibers. J Cell Sci. 1991;99:99–106.
26. Fuchigami T, Kawamura R, Kitamoto Y, Nakagawa M, Namiki Y. Ferromagnetic FePt-nanoparticles/polycation hybrid capsules designed for a magnetically guided drug delivery system. Langmuir. 2011;27:2923-8.
27. Namiki Y, Matsunuma S, Inoue T, Koido S, Tsubota A, Kuse Y, Tada N. Magnetic nanostructures for biomedical application. In: Masuda Y, editor. Nanocrystal. Rijeka: Sciyo; 2011. p. 349–72.
28. Luo L, Liu J, Wang Z, Yang X, Dong S, Wang E. Fabrication of layer-by-layer deposited multilayer films containing DNA and its interaction with methyl green. Biophys Chem. 2001;94:11–22.
29. Caruso F, Furlong DN, Ariga K, Ichinose I, Kunitake T. Characterization of polyelectrolyte-protein multilayer films by atomic force microscopy, scanning electron microscopy, and fourier transform infrared reflection-absorption spectroscopy. Langmuir. 1998;14:4559–65.
30. Vanhoe H, Vandecasteele C, Versieck J, Dams R. Determination of iron, cobalt, copper, zinc, rubidium, molybdenum and cesium in human serum by inductively coupled plasma mass spectrometry. Anal Chem. 1989;61:1851–7.
31. Bulte JW, De Cuyper M. Magnetoliposomes as contrast agents. In: Abelson, JN.; Simon, MI. Editors. Liposomes. Elsevier, USA: Academic Press; 2003, p.175–98.
32. Faustino PJ, Yang Y, Progar JJ, Brownell CR, Sadrieh N, May JC, *et al.* Quantitative determination of cesium binding to ferric hexacyanoferrate: Prussian blue. J Pharm Biomed Anal. 2008;47:114–25.
33. Yang Y, Faustino PJ, Progar JJ, Brownell CR, Sadrieh N, May JC, *et al.* Quantitative determination of thallium binding to ferric hexacyanoferrate: Prussian blue. Int J Pharm. 2008;353:187–94.
34. Pajerowski DM, Andrus MJ, Gardner JE, Knowles ES, Meisel MW, Talham DR. Persistent photoinduced magnetism in heterostructures of Prussian blue analogues. J Am Chem Soc. 2010;132:4058–9.
35. Zhang XQ, Gong SW, Zhan Y, Yang T, Wang CY, Gu N. Prussian blue modified iron oxide magnetic nanoparticles and their high peroxidase-like activity. J Mater Chem. 2010;20:5110–6.
36. Wang H, Huang Y. Prussian-blue-modified iron oxide magnetic nanoparticles as effective peroxidase-like catalysts to degrade methylene blue with H(2)O(2). J Hazard Mater. 2011;191:163–9.
37. Urban I, Ratcliffe NM, Duffield JR, Elder GR, Patton D. Functionalized paramagnetic nanoparticles for waste water treatment. Chem Commun. 2010;46:4583–5.
38. Smith JT. The influence of hot particle contamination on (90)Sr and (137)Cs transfers to milk and on time-integrated ingestion doses. J Environ Radioact. 2009;100:322–8.